ELSEVIER

SCIENCE DIRECT®

PHYSICS LETTERS B

Physics Letters B 581 (2004) 19–30

www.elsevier.com/locate/physletb

Search for colour singlet and colour reconnection effects in hadronic Z decays at LEP

L3 Collaboration

P. Achard [t], O. Adriani [q], M. Aguilar-Benitez [x], J. Alcaraz [x], G. Alemanni [v], J. Allaby [r], A. Aloisio [ab], M.G. Alviggi [ab], H. Anderhub [at], V.P. Andreev [f,ag], F. Anselmo [h], A. Arefiev [aa], T. Azemoon [c], T. Aziz [i], P. Bagnaia [al], A. Bajo [x], G. Baksay [y], L. Baksay [y], S.V. Baldew [b], S. Banerjee [i], Sw. Banerjee [d], A. Barczyk [at,ar], R. Barillère [r], P. Bartalini [v], M. Basile [h], N. Batalova [aq], R. Battiston [af], A. Bay [v], F. Becattini [q], U. Becker [m], F. Behner [at], L. Bellucci [q], R. Berbeco [c], J. Berdugo [x], P. Berges [m], B. Bertucci [af], B.L. Betev [at], M. Biasini [af], M. Biglietti [ab], A. Biland [at], J.J. Blaising [d], S.C. Blyth [ah], G.J. Bobbink [b], A. Böhm [a], L. Boldizsar [l], B. Borgia [al], S. Bottai [q], D. Bourilkov [at], M. Bourquin [t], S. Braccini [t], J.G. Branson [an], F. Brochu [d], J.D. Burger [m], W.J. Burger [af], X.D. Cai [m], M. Capell [m], G. Cara Romeo [h], G. Carlino [ab], A. Cartacci [q], J. Casaus [x], F. Cavallari [al], N. Cavallo [ai], C. Cecchi [af], M. Cerrada [x], M. Chamizo [t], Y.H. Chang [av], M. Chemarin [w], A. Chen [av], G. Chen [g], G.M. Chen [g], H.F. Chen [u], H.S. Chen [g], G. Chiefari [ab], L. Cifarelli [am], F. Cindolo [h], I. Clare [m], R. Clare [ak], G. Coignet [d], N. Colino [x], S. Costantini [al], B. de la Cruz [x], S. Cucciarelli [af], J.A. van Dalen [ad], R. de Asmundis [ab], P. Déglon [t], J. Debreczeni [l], A. Degré [d], K. Dehmelt [y], K. Deiters [ar], D. della Volpe [ab], E. Delmeire [t], P. Denes [aj], F. DeNotaristefani [al], A. De Salvo [at], M. Diemoz [al], M. Dierckxsens [b], C. Dionisi [al], M. Dittmar [at], A. Doria [ab], M.T. Dova [j,5], D. Duchesneau [d], M. Duda [a], B. Echenard [t], A. Eline [r], A. El Hage [a], H. El Mamouni [w], A. Engler [ah], F.J. Eppling [m], P. Extermann [t], M.A. Falagan [x], S. Falciano [al], A. Favara [ae], J. Fay [w], O. Fedin [ag], M. Felcini [at], T. Ferguson [ah], H. Fesefeldt [a], E. Fiandrini [af], J.H. Field [t], F. Filthaut [ad], P.H. Fisher [m], W. Fisher [aj], I. Fisk [an], G. Forconi [m], K. Freudenreich [at], C. Furetta [z], Yu. Galaktionov [aa,m], S.N. Ganguli [i], P. Garcia-Abia [x], M. Gataullin [ae], S. Gentile [al], S. Giagu [al], Z.F. Gong [u], G. Grenier [w], O. Grimm [at], M.W. Gruenewald [p], M. Guida [am], R. van Gulik [b], V.K. Gupta [aj], A. Gurtu [i], L.J. Gutay [aq], D. Haas [e], D. Hatzifotiadou [h], T. Hebbeker [a], A. Hervé [r], J. Hirschfelder [ah], H. Hofer [at], M. Hohlmann [y], G. Holzner [at], S.R. Hou [av], Y. Hu [ad], B.N. Jin [g], L.W. Jones [c], P. de Jong [b], I. Josa-Mutuberría [x], D. Käfer [a], M. Kaur [n], M.N. Kienzle-Focacci [t], J.K. Kim [ap], J. Kirkby [r], W. Kittel [ad], A. Klimentov [m,aa], A.C. König [ad], M. Kopal [aq],

doi:10.1016/j.physletb.2003.12.003

V. Koutsenko [m,aa], M. Kräber [at], R.W. Kraemer [ah], A. Krüger [as], A. Kunin [m], P. Ladron de Guevara [x], I. Laktineh [w], G. Landi [q], M. Lebeau [r], A. Lebedev [m], P. Lebrun [w], P. Lecomte [at], P. Lecoq [r], P. Le Coultre [at], J.M. Le Goff [r], R. Leiste [as], M. Levtchenko [z], P. Levtchenko [ag], C. Li [u], S. Likhoded [as], C.H. Lin [av], W.T. Lin [av], F.L. Linde [b], L. Lista [ab], Z.A. Liu [g], W. Lohmann [as], E. Longo [al], Y.S. Lu [g], C. Luci [al], L. Luminari [al], W. Lustermann [at], W.G. Ma [u], L. Malgeri [t], A. Malinin [aa], C. Maña [x], J. Mans [aj], J.P. Martin [w], F. Marzano [al], K. Mazumdar [i], R.R. McNeil [f], S. Mele [r,ab], L. Merola [ab], M. Meschini [q], W.J. Metzger [ad], A. Mihul [k], H. Milcent [r], G. Mirabelli [al], J. Mnich [a], G.B. Mohanty [i], G.S. Muanza [w], A.J.M. Muijs [b], B. Musicar [an], M. Musy [al], S. Nagy [o], S. Natale [t], M. Napolitano [ab], F. Nessi-Tedaldi [at], H. Newman [ae], A. Nisati [al], T. Novak [ad], H. Nowak [as], R. Ofierzynski [at], G. Organtini [al], I. Pal [aq], C. Palomares [x], P. Paolucci [ab], R. Paramatti [al], G. Passaleva [q], S. Patricelli [ab], T. Paul [j], M. Pauluzzi [af], C. Paus [m], F. Pauss [at], M. Pedace [al], S. Pensotti [z], D. Perret-Gallix [d], B. Petersen [ad], D. Piccolo [ab], F. Pierella [h], M. Pioppi [af], P.A. Piroué [aj], E. Pistolesi [z], V. Plyaskin [aa], M. Pohl [t], V. Pojidaev [q], J. Pothier [r], D. Prokofiev [ag], J. Quartieri [am], G. Rahal-Callot [at], M.A. Rahaman [i], P. Raics [o], N. Raja [i], R. Ramelli [at], P.G. Rancoita [z], R. Ranieri [q], A. Raspereza [as], P. Razis [ac], D. Ren [at], M. Rescigno [al], S. Reucroft [j], S. Riemann [as], K. Riles [c], B.P. Roe [c], L. Romero [x], A. Rosca [as], S. Rosier-Lees [d], S. Roth [a], C. Rosenbleck [a], J.A. Rubio [r], G. Ruggiero [q], H. Rykaczewski [at], A. Sakharov [at], S. Saremi [f], S. Sarkar [al], J. Salicio [r], E. Sanchez [x], C. Schäfer [r], V. Schegelsky [ag], H. Schopper [au], D.J. Schotanus [ad], C. Sciacca [ab], L. Servoli [af], S. Shevchenko [ae], N. Shivarov [ao], V. Shoutko [m], E. Shumilov [aa], A. Shvorob [ae], D. Son [ap], C. Souga [w], P. Spillantini [q], M. Steuer [m], D.P. Stickland [aj], B. Stoyanov [ao], A. Straessner [r], K. Sudhakar [i], G. Sultanov [ao], L.Z. Sun [u], S. Sushkov [a], H. Suter [at], J.D. Swain [j], Z. Szillasi [y,3], X.W. Tang [g], P. Tarjan [o], L. Tauscher [e], L. Taylor [j], B. Tellili [w], D. Teyssier [w], C. Timmermans [ad], Samuel C.C. Ting [m], S.M. Ting [m], S.C. Tonwar [i], J. Tóth [l], C. Tully [aj], K.L. Tung [g], J. Ulbricht [at], E. Valente [al], R.T. Van de Walle [ad], R. Vasquez [aq], V. Veszpremi [y], G. Vesztergombi [l], I. Vetlitsky [aa], D. Vicinanza [am], G. Viertel [at], S. Villa [ak], M. Vivargent [d], S. Vlachos [e], I. Vodopianov [y], H. Vogel [ah], H. Vogt [as], I. Vorobiev [ah,aa], A.A. Vorobyov [ag], M. Wadhwa [e], Q. Wang [ad], X.L. Wang [u], Z.M. Wang [u], M. Weber [a], P. Wienemann [a], H. Wilkens [ad], S. Wynhoff [aj], L. Xia [ae], Z.Z. Xu [u], J. Yamamoto [c], B.Z. Yang [u], C.G. Yang [g], H.J. Yang [c], M. Yang [g], S.C. Yeh [aw], An. Zalite [ag], Yu. Zalite [ag], Z.P. Zhang [u], J. Zhao [u], G.Y. Zhu [g], R.Y. Zhu [ae], H.L. Zhuang [g], A. Zichichi [h,r,s], B. Zimmermann [at], M. Zöller [a]

[a] *III. Physikalisches Institut, RWTH, D-52056 Aachen, Germany* [1]
[b] *National Institute for High Energy Physics, NIKHEF, and University of Amsterdam, NL-1009 DB Amsterdam, The Netherlands*
[c] *University of Michigan, Ann Arbor, MI 48109, USA*
[d] *Laboratoire d'Annecy-le-Vieux de Physique des Particules, LAPP, IN2P3-CNRS, BP 110, F-74941 Annecy-le-Vieux cedex, France*
[e] *Institute of Physics, University of Basel, CH-4056 Basel, Switzerland*

[f] Louisiana State University, Baton Rouge, LA 70803, USA
[g] Institute of High Energy Physics, IHEP, 100039 Beijing, China [6]
[h] University of Bologna and INFN-Sezione di Bologna, I-40126 Bologna, Italy
[i] Tata Institute of Fundamental Research, Mumbai (Bombay) 400 005, India
[j] Northeastern University, Boston, MA 02115, USA
[k] Institute of Atomic Physics and University of Bucharest, R-76900 Bucharest, Romania
[l] Central Research Institute for Physics of the Hungarian Academy of Sciences, H-1525 Budapest 114, Hungary [2]
[m] Massachusetts Institute of Technology, Cambridge, MA 02139, USA
[n] Panjab University, Chandigarh 160 014, India
[o] KLTE-ATOMKI, H-4010 Debrecen, Hungary [3]
[p] Department of Experimental Physics, University College Dublin, Belfield, Dublin 4, Ireland
[q] INFN Sezione di Firenze and University of Florence, I-50125 Florence, Italy
[r] European Laboratory for Particle Physics, CERN, CH-1211 Geneva 23, Switzerland
[s] World Laboratory, FBLJA Project, CH-1211 Geneva 23, Switzerland
[t] University of Geneva, CH-1211 Geneva 4, Switzerland
[u] Chinese University of Science and Technology, USTC, Hefei, Anhui 230 029, China [6]
[v] University of Lausanne, CH-1015 Lausanne, Switzerland
[w] Institut de Physique Nucléaire de Lyon, IN2P3-CNRS, Université Claude Bernard, F-69622 Villeurbanne, France
[x] Centro de Investigaciones Energéticas, Medioambientales y Tecnológicas, CIEMAT, E-28040 Madrid, Spain [4]
[y] Florida Institute of Technology, Melbourne, FL 32901, USA
[z] INFN-Sezione di Milano, I-20133 Milan, Italy
[aa] Institute of Theoretical and Experimental Physics, ITEP, Moscow, Russia
[ab] INFN-Sezione di Napoli and University of Naples, I-80125 Naples, Italy
[ac] Department of Physics, University of Cyprus, Nicosia, Cyprus
[ad] University of Nijmegen and NIKHEF, NL-6525 ED Nijmegen, The Netherlands
[ae] California Institute of Technology, Pasadena, CA 91125, USA
[af] INFN-Sezione di Perugia and Università Degli Studi di Perugia, I-06100 Perugia, Italy
[ag] Nuclear Physics Institute, St. Petersburg, Russia
[ah] Carnegie Mellon University, Pittsburgh, PA 15213, USA
[ai] INFN-Sezione di Napoli and University of Potenza, I-85100 Potenza, Italy
[aj] Princeton University, Princeton, NJ 08544, USA
[ak] University of California, Riverside, CA 92521, USA
[al] INFN-Sezione di Roma and University of Rome, "La Sapienza", I-00185 Rome, Italy
[am] University and INFN, Salerno, I-84100 Salerno, Italy
[an] University of California, San Diego, CA 92093, USA
[ao] Bulgarian Academy of Sciences, Central Laboratory of Mechatronics and Instrumentation, BU-1113 Sofia, Bulgaria
[ap] The Center for High Energy Physics, Kyungpook National University, 702-701 Taegu, Republic of Korea
[aq] Purdue University, West Lafayette, IN 47907, USA
[ar] Paul Scherrer Institut, PSI, CH-5232 Villigen, Switzerland
[as] DESY, D-15738 Zeuthen, Germany
[at] Eidgenössische Technische Hochschule, ETH Zürich, CH-8093 Zürich, Switzerland
[au] University of Hamburg, D-22761 Hamburg, Germany
[av] National Central University, Chung-Li, Taiwan, ROC
[aw] Department of Physics, National Tsing Hua University, Taiwan, ROC

Received 16 July 2003; received in revised form 11 November 2003; accepted 8 December 2003

Editor: L. Rolandi

Abstract

A search is performed in symmetric 3-jet hadronic Z-decay events for evidence of colour singlet production or colour reconnection effects. Asymmetries in the angular separation of particles are found to be sensitive indicators of such effects. Upper limits on the level of colour singlet production or of colour reconnection effects are established for a variety of models.

1. Introduction

The term 'rapidity gaps' denotes regions of angular phase space devoid of particles. They are expected in low-p_T diffractive processes, where separate colour singlet hadronic systems are produced, well separated in phase space and associated with either the target or projectile particles. Events containing large rapidity gaps, attributed to colour singlet exchange or colour reconnection effects, are also observed, in association with high-p_T jet production, at HERA [1] and at the TEVATRON [2]. As shown in Fig. 1(a) and (b), by crossing symmetry, similar gaps may be expected in three-jet hadronic Z decays at LEP. The corresponding diagram has four final state partons, but, because of its generally low energy, the two jets associated with the colour singlet object are typically unresolved.

Large rapidity gaps are observed in $\simeq 10\%$ and 1–2% of events with two high-p_T jets at HERA and at the TEVATRON, respectively. In electron–hadron or hadron–hadron collisions particles produced by the spectator partons of the underlying event frequently destroy large rapidity gaps associated with the primary hard scattering process. The associated 'gap survival probability' is estimated [3] to be about 20% at the TEVATRON. An advantage of the Z-decay study is the absence of this suppression factor, as there is no underlying event. A disadvantage is that the maximum possible size of the angular gap is smaller for Z decays compared to ep or $p\bar{p}$ collisions. Particle and energy flow in the inter-jet regions have been studied [4] using three-jet events in e^+e^- annihilations. These studies revealed that the region between two-quark jets have lower particle and energy flows relative to naïve expectation from independent fragmentation models. This was also observed in studies which compared three-jet events with two-jet events having a hard photon in the final state [5].

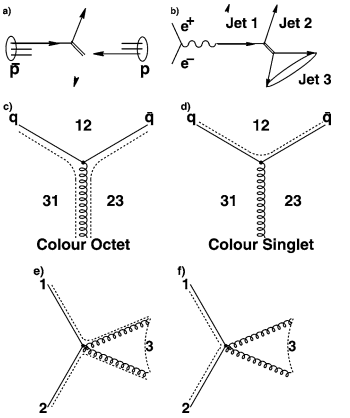

Fig. 1. Schematic diagram of colour exchange. Colour singlet propagators are indicated by double lines in (a) $p\bar{p}$ and in (b) e^+e^- reactions. The e^+e^- diagram is derived by crossing the incoming quark line in the $p\bar{p}$ diagram. Colour flow is shown by dashed lines for (c) COP and (d) CSP in 3-jet events from e^+e^- annihilation and also (e) without and (f) with colour reconnection.

The analysis presented in this Letter is performed with hadronic Z-decay events recorded by the L3 detector [6] using 75.14 pb^{-1} of data from the 1994–1995 Z-pole data taking periods. In the new method presented here, a search is performed for gaps in angular phase space in symmetric 3-jet hadronic Z-decay events. The method exploits the different particle flows between quark and antiquark jets and either the quark or antiquark jet and the gluon jet. After removing particles near to the jet cores, angular gaps between particles in the inter-jet regions are analysed, and various asymmetry variables are formed, as detailed below.

Studies of rapidity gaps in hadronic Z decays using as variable the pseudo-rapidity of particles relative to the thrust axis were previously reported [7]. A recent study [8] used the axes of tagged gluon jets. The analysis presented in this Letter, based on global event variables, is complementary to this study in the sense that the jet cores are excluded from the analysis so as to minimise fragmentation effects whereas previous analyses rather used rapidity gaps as a tool to investigate the details of gluon fragmentation [8].

The present analysis extends the notion of comparing particle and energy flow in the region opposite to the quark jets as well as in the region between the two-quark jets by introducing new asymmetry variables

[1] Supported by the German Bundesministerium für Bildung, Wissenschaft, Forschung und Technologie.

[2] Supported by the Hungarian OTKA fund under Contract Nos. T019181, F023259 and T037350.

[3] Also supported by the Hungarian OTKA fund under Contract No. T026178.

[4] Supported also by the Comisión Interministerial de Ciencia y Tecnología.

[5] Also supported by CONICET and Universidad Nacional de La Plata, CC 67, 1900 La Plata, Argentina.

[6] Supported by the National Natural Science Foundation of China.

that are sensitive to the relative difference in colour flow between all the inter-jet regions.

A first application of these asymmetries is to exploit differences in colour flow between events where colour singlet systems are produced (CSP) and conventional gluon colour octet production (COP). As shown in Fig. 1(c), in COP, colour flow is present between the qg and $\bar{q}g$ gaps and is inhibited by destructive interference in the $q\bar{q}$ gap. As shown in Fig. 1(d), the colour string in the CSP is drawn between the quark and the antiquark so that an appreciable colour flow occurs also in the $q\bar{q}$ gap.

A second application is to investigate colour reconnection (CR) effects. Partons originating from a hard scattering process are eventually transformed into hadrons and this hadronisation process requires specification of the colour flow pattern among the partons. In the simplest models, the colour flow associated with the final state partons is fixed during the hard scattering process. However, there may be subsequent rearrangement of the colour flow. At the perturbative level this requires the exchange of at least two gluons between the partons. Coloured strings, normally stretched between a quark and a gluon as shown in Fig. 1(e), can be rearranged in the colour reconnection picture so as to create colour singlet quark pair in association with a colour singlet gluon pair, whose colour strings then hadronise independently, as shown in Fig. 1(f). To study CR effects, the GAL [9] model as well as CR as implemented in ARIADNE [10] and HERWIG [11] are considered.

Studies of the determination of the W boson mass using fully hadronic W-pair decays, indicate CR effects as the dominant source of theoretical systematic uncertainty. If the same CR algorithm is valid for both Z- and W-pair decays, limits on the level of CR effects, established experimentally at the Z-pole, can be used to constrain the systematic uncertainty on the W-mass determination. The present analysis is thus complementary to the direct measurement of CR effects in hadronic decays of W-pairs [12].

2. Event and particle selection

Well balanced hadronic Z-decay events are selected by cuts on the number of calorimetric clusters with energy greater than 100 MeV, N_{cluster}, on the total energy observed in the calorimeters, E_{vis}, the energy imbalance along the beam direction, $E_{\parallel}$, and the energy imbalance in the plane perpendicular to the beam direction, $E_{\perp}$. The cut on the number of calorimetric clusters rejects low multiplicity events such as $\tau^-\tau^+$ final states. About two million hadronic Z-decay candidates are selected.

Symmetric three-jet events with a jet–jet angular separation of about 120° are then selected using the JADE algorithm [13], with the jet resolution parameter set to 0.05. The angles between jets i and j, ϕ_{ij}, are required to be within ±30° of the symmetric topology. Using the selection criteria:

$$N_{\text{cluster}} > 12, \qquad 0.6 < \frac{E_{\text{vis}}}{\sqrt{s}} < 1.4,$$

$$\frac{E_{\parallel}}{E_{\text{vis}}} < 0.40, \qquad \frac{E_{\perp}}{E_{\text{vis}}} < 0.40,$$

$$\phi_{12}, \phi_{23}, \phi_{31} \in [90^\circ, 150^\circ],$$

where $\sqrt{s}$ is the centre-of-mass energy, about 70000 three-jet events are obtained. In order to distinguish quark jets from gluon or colour singlet jets, the energy-ordered quark jets are tagged by cuts on the b-tag discriminant:[7]

$$D_1^{\text{jet}} > 1.25, \qquad D_2^{\text{jet}} > 1.25, \qquad D_3^{\text{jet}} < 1.5.$$

As shown in Fig. 2, these cuts strongly enhance the gluon fraction in jet 3. This selection tags 2668 events with a gluon purity of 78%.

To study the particle flow, calorimetric clusters are selected which satisfy at least one of the following criteria:

- energy greater than 100 MeV in the electromagnetic calorimeter (ECAL) and at least 900 MeV in the hadron calorimeter (HCAL);
- energy greater than 100 MeV in the ECAL with a minimum of 2 crystals hit;
- energy greater than 1800 MeV in the HCAL alone.

[7] The jet b-tag discriminant of jet i, containing n tracks, is defined as: $D_i^{\text{jet}} = -\log_{10} P$ where $P = P_i^n \sum_{j=0}^{n-1} (-\ln P_i^n)^j / j!$ and $P_i^n = \prod_{j=1}^{n} P_j$. Here, P_j is the probability that the jth track in the jet originates at the primary vertex.

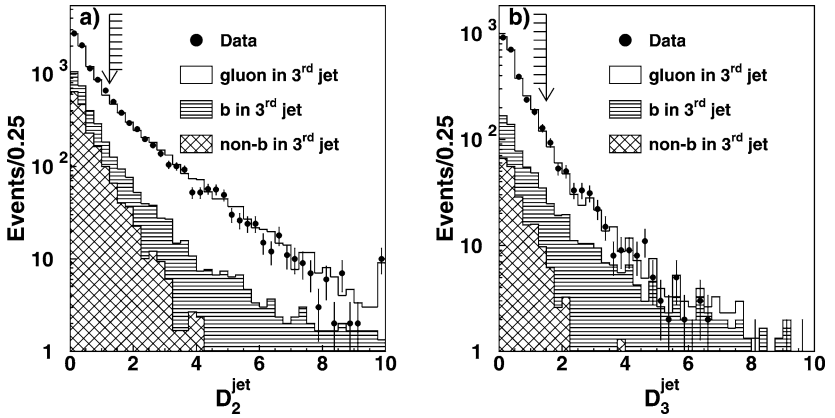

Fig. 2. b-tag discriminant plots for energy-ordered jets: (a) for jet 2 and (b) for jet 3. Vertical arrows represent the cuts.

These cuts reject noisy clusters and take into account different thresholds in the calorimeters. The distributions of the cluster multiplicity with these selection criteria show good agreement between data and Monte Carlo, with residual differences below 2.5%.

3. Monte Carlo samples

The JETSET parton shower (PS) Monte Carlo program [14] is used to model COP. Two simple models are used to simulate the expected colour flow in CSP: events of type $q\bar{q}\gamma$ are generated with a photon effective mass as in the gluon jet mass distribution. In the first model, CS1, the photon is replaced by a boosted di-quark jet. In the second model, CS2, the photon is replaced by a gluon fragmenting independently. The total particle multiplicity for both these models agree with JETSET within ± 1 unit.

For CR studies, the GAL model, implemented in the PYTHIA Monte Carlo program [15], uses a default value of 0.1 for the colour recombination parameter, R_0. This value is obtained [9] by fitting the model to H1 data on the diffractive proton structure function. For this study the fragmentation parameters of the model are tuned to Z-decay data[8] for three different values of the colour recombination parameter: $R_0 = 0.05, 0.1, 0.2$. The ARIADNE and HERWIG generators, with and without CR, are also tuned to Z-decay data to determine their basic fragmentation parameters. The colour reconnection probability in HERWIG is set to its default value of 1/9 [11]. Similarly, the parameters affecting colour reconnection in ARIADNE are kept at their default values [10], $\texttt{para}(26) = 9$ and $\texttt{para}(28) = 0$.

4. Inter-jet gap asymmetries

After selection of three-jet events, the particle momenta are projected onto the event plane defined by the two most energetic jets. In order to minimise the bias from jet fragmentation, particles in a cone of 15° half-angle about the jet axis direction are excluded from the analysis. The angles of the remaining particles are measured in this plane with respect to the most energetic jet. In order to achieve uniformity in the event-to-event comparison, these angles are rescaled so as to align jets at 0°, 120° and 240°. This is achieved by scaling the angle of a particle to its nearest jet by the ratio between 120° and the opening angle of the two jets between which the particle is located.

[8] The QCD models are tuned using several global event shape distributions at $\sqrt{s} \approx m_Z$: the minor on the narrow side [16], the jet resolution parameter for the transition from 2- to 3-jet in the JADE [13] algorithm, the fourth Fox–Wolfram moment [17] and the charged particle multiplicity. For models implemented in PYTHIA, the tuned parameters are the QCD cut-off parameter, Λ, and the string fragmentation parameters, b and σ_Q, affecting longitudinal and transverse components of the hadron momenta. In HERWIG, the QCD cut-off parameter and the parameters controlling hadronisation, CLMAX (maximum cluster mass) and CLPOW (the power of the mass in the expression for the cluster splitting criterion) are tuned.

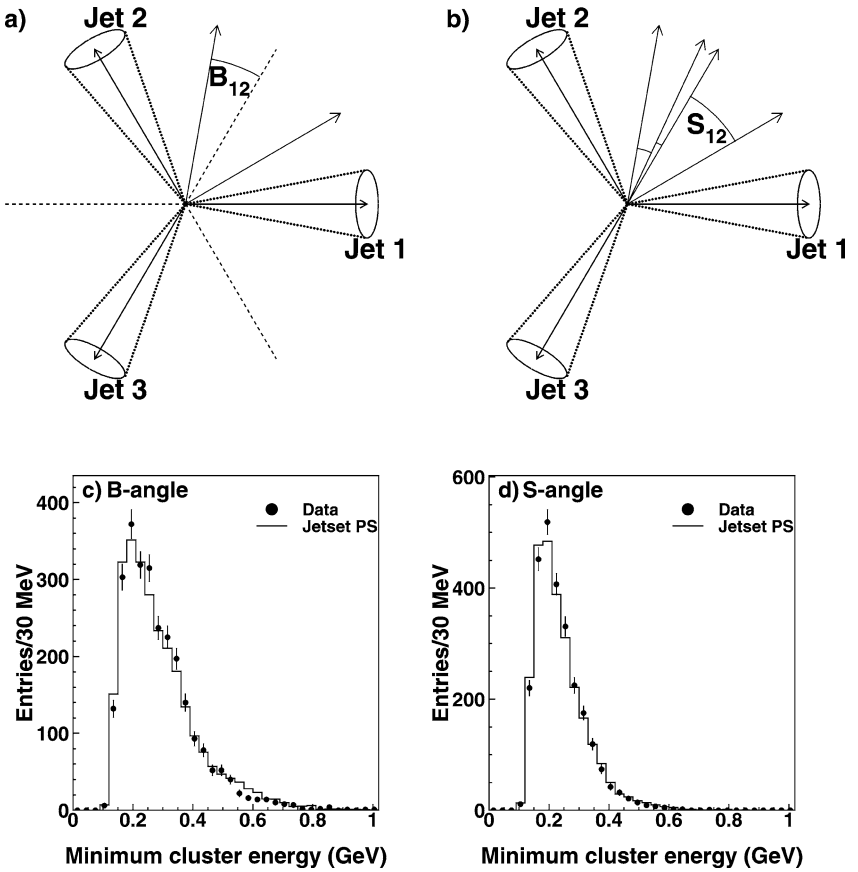

Fig. 3. Definition of (a) minimum angle relative to the gap bisector and (b) the maximum separation angle between adjacent particles for the case of four particles in the sensitive region of gap 12. Only particles outside the $\pm 15^\circ$ cones around the jet axes are considered. Distributions of the minimum energy of clusters used to define (c) the bisector angle and (d) the maximum separation in selected symmetric three-jet events compared to the JETSET PS prediction.

Two gap angle definitions are used [18], as shown in Fig. 3(a) and (b): the minimum angle, B_{ij}, of a particle measured from the bisector in the gap ij, and the maximum separation angle, S_{ij}, between adjacent particles in the gap. In Fig. 3(c) and (d) the minimum energy of the calorimetric clusters used to define the bisector angle or the maximum separation angle is compared with the JETSET prediction. Good agreement is obtained, showing that the contribution of soft particles, to which rapidity gap distributions are particularly sensitive, is well simulated.

The angular asymmetry in gap 12 from the B_{ij} angles is defined as

$$A_{12}^{B} = \frac{-B_{12} + B_{23} + B_{31}}{B_{12} + B_{23} + B_{31}}.$$

Asymmetries are also defined from the S_{ij} angles as

$$A_{12}^{S} = \frac{-S_{12} + S_{23} + S_{31}}{S_{12} + S_{23} + S_{31}}.$$

The other gap asymmetries: A_{ij}^{B}, A_{ij}^{S}, with $ij = 23, 31$ are defined in a similar way.

Reduced colour flow and thereby larger separation for CSP in gaps 23, 31 with respect to gap 12, should thus make A_{12}^{B} and A_{12}^{S} peak more strongly at positive values for CSP than for COP. The 23 and 31 gap asymmetries of each event are averaged to yield the 'qg' asymmetries shown below.

The angular asymmetry distributions are corrected for detector effects and initial and final state photon radiation using bin-by-bin correction factors obtained from events generated with the JETSET parton

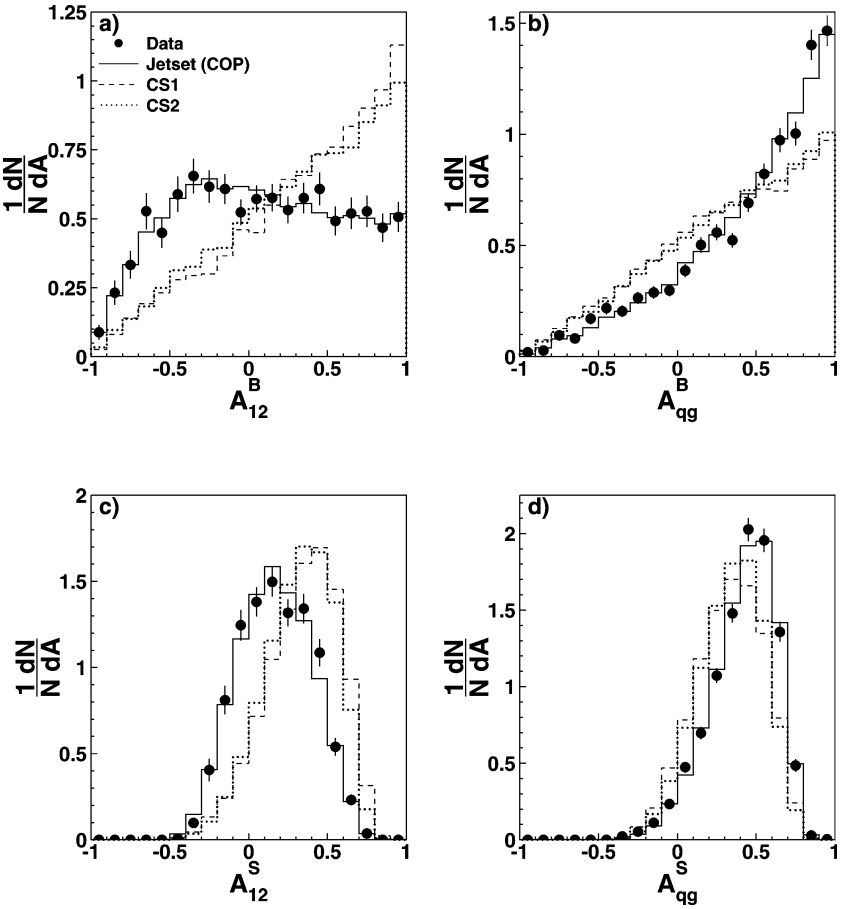

Fig. 4. (a) and (b) minimum bisector angle gap asymmetries, and (c) and (d) maximum separation gap asymmetries for gaps 12 and qg, respectively, compared to colour singlet and colour octet models.

shower Monte Carlo program and processed through L3 detector simulation [19]. The bin sizes are chosen sufficiently large that migration effects are negligible. The correction factors are defined as the ratio of generated particle-level distributions, considering all charged and neutral particles, without energy cuts, to the same distributions after detector simulation. The particle-level distributions take into account the gluon jet identification probability and have a quark flavour composition corresponding to $\sqrt{s} \approx m_Z$. These bin-by-bin correction factors for the angular asymmetries typically lie in the range of $\pm 20\%$.

The particle-level angular asymmetry distributions of the selected symmetric three-jet events, normalised to unit area, are compared to different models, in Figs. 4, 5 and 6.

Table 1
Systematic uncertainties on the measurements of the asymmetry variables

	Systematic uncertainties (%)			
Variable	Detector	b-tag	Monte Carlo	Total
A_{12}^B	5.2	4.8	2.5	7.5
A_{qg}^B	5.9	3.2	2.5	7.1
A_{12}^S	6.6	8.1	2.5	10.8
A_{qg}^S	2.8	4.0	2.5	5.5

Fractional bin-by-bin systematic uncertainties are estimated by repeating the analysis using clusters obtained by combining calorimetric clusters with tracks, as used, for instance, in Ref. [12]. A variation between 2 and 5% is observed. Furthermore, the cuts on the

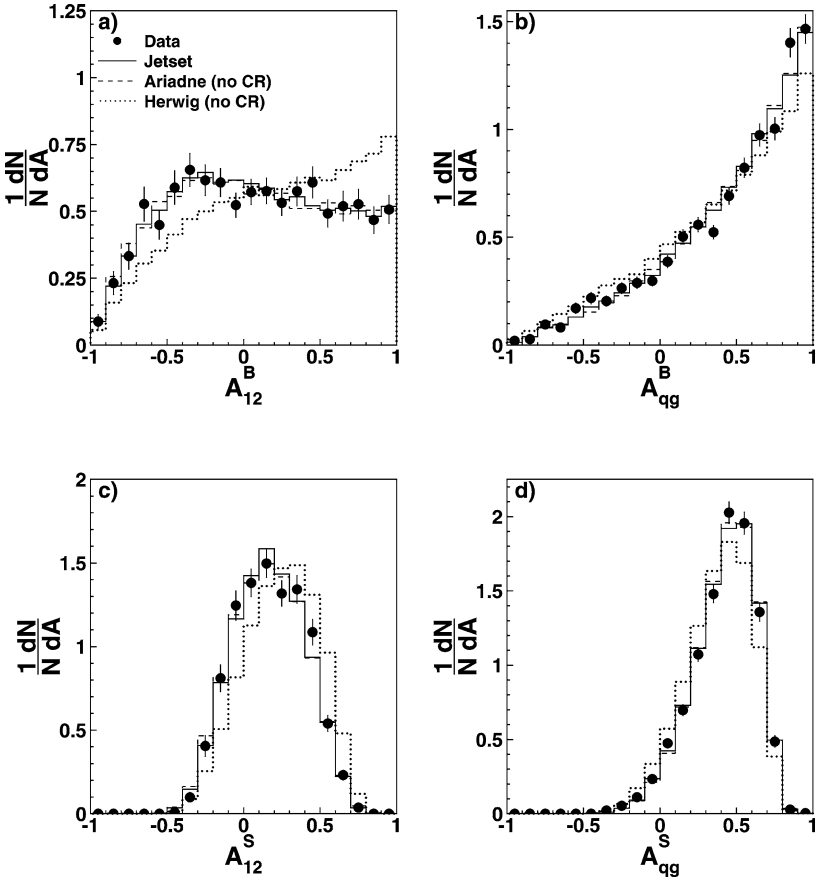

Fig. 5. (a) and (b) minimum bisector angle gap asymmetries, and (c) and (d) maximum separation gap asymmetries for gaps 12 and qg, respectively, compared to models without CR effects.

b-tag discriminant are changed so that the gluon purity varies by $\pm 10\%$, which results in systematic uncertainties between 3 and 8%. Finally, the residual 2.5% difference between data and Monte Carlo discussed above is included. These uncertainties are added in quadrature and are summarised in Table 1. The systematic uncertainty due to a change in the jet cone angle cut from $\pm 15^\circ$ to $\pm 20^\circ$ is found to be negligible.

5. Limits on colour singlet production

As shown in Fig. 4, the data are in good agreement with the COP model. The high discrimination power of the angular asymmetries between the COP and CSP models is also evident. A quantitative comparison is given in Table 2. The COP model is in good agreement with the data. The CSP models are clearly excluded. As a cross-check, the analysis is repeated us-

Table 2
Values of χ^2 obtained from the comparison of the data distributions to colour octet and colour singlet models. For COP the corresponding confidence levels are given in parentheses. For the CSP models all confidence levels are less than 10^{-30}. The χ^2 values include systematic uncertainties

	χ^2 for			
Variable	COP	CS1	CS2	d.o.f.
A_{12}^{B}	6.4 (0.99)	356	262	19
A_{qg}^{B}	15.9 (0.60)	238	189	18
A_{12}^{S}	4.8 (0.94)	1081	524	11
A_{qg}^{S}	6.7 (0.88)	334	266	12

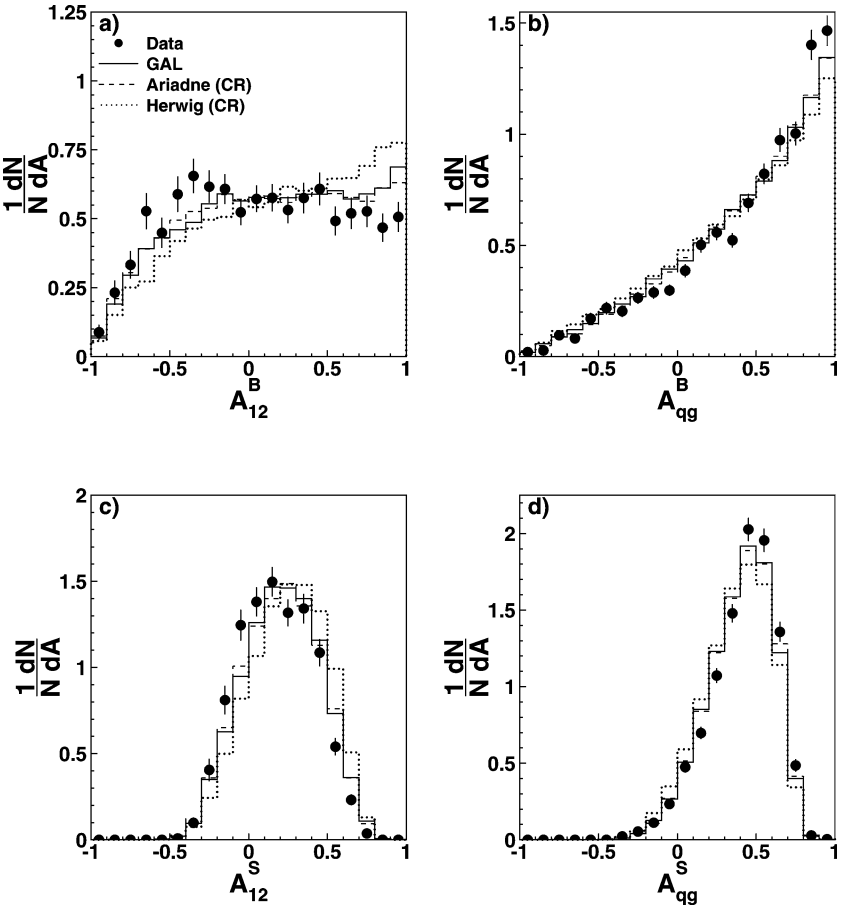

Fig. 6. (a) and (b) minimum bisector angle gap asymmetries, and (c) and (d) maximum separation gap asymmetries for gaps 12 and qg, respectively, compared to models with CR effects.

ing the DURHAM $k_\perp$ algorithm [20] with $y_{\text{cut}} = 0.01$ and $y_{\text{cut}} = 0.02$ instead of the JADE algorithm, effectively defining an independent set of asymmetries. No significant changes are observed.

The asymmetry distributions are fitted to a combination of COP and CSP contributions. This is done by minimising a χ^2 function defined as

$$\chi^2(r) = \sum_i \frac{[f^i_{\text{data}} - r f^i_{\text{CSP}} - (1-r) f^i_{\text{COP}}]^2}{(\sigma^i_{\text{stat}})^2 + (\sigma^i_{\text{syst}})^2},$$

where f^i is the content of the ith bin of the distribution, r is the fraction of the CSP component and contributions from both statistical, σ^i_{stat}, and systematic, σ^i_{syst}, uncertainties are included.

Good fits are obtained for all the asymmetry distributions. For the variable A^S_{12}, which Monte Carlo studies show to be the most sensitive one, the fit gives $r = 0.015 \pm 0.024(\text{stat}) \pm 0.018(\text{syst})$ with $\chi^2/\text{d.o.f.} = 4.5/11$ for the CS1 model $r = 0.025 \pm 0.031(\text{stat}) \pm 0.029(\text{syst})$ with $\chi^2/\text{d.o.f.} = 4.4/11$ for the CS2 model. All the fits give a fraction of events due to CSP consistent with zero. The fits to the distributions are then used to obtain a 95% confidence level (CL) upper bound on the fraction of CSP events. The asymmetry variables A^B_{12} and A^B_{qg} are independent, as are A^S_{12} and A^S_{qg}. These pairs of variables are thus combined in the fits. Upper bounds of 6.7 and 10.2% for the CS1 and CS2 models, respectively, are found using A^S_{12} and A^S_{qg}. Using A^B_{12} and A^B_{qg} yields slightly weaker limits.

Table 3
χ^2 confidence levels obtained from the comparison of the data distributions to different models with and without CR. Low confidence levels are rounded to the nearest order of magnitude

	No CR			CR		
Variable	JETSET	ARIADNE	HERWIG	GAL	ARIADNE	HERWIG
A_{12}^B	0.99	0.93	10^{-9}	0.04	0.27	10^{-11}
A_{qg}^B	0.60	0.13	10^{-8}	10^{-4}	0.02	10^{-8}
A_{12}^S	0.94	0.80	10^{-24}	10^{-8}	10^{-6}	10^{-30}
A_{qg}^S	0.88	0.78	10^{-8}	0.03	0.07	10^{-11}

6. Limits on colour reconnection effects

The particle-level angular asymmetry distributions are compared to the predictions of several different Monte Carlo models in Figs. 5 and 6. These include the 'no CR' models JETSET, ARIADNE and HERWIG as well as the GAL model and the CR versions of ARIADNE and HERWIG. The χ^2 confidence levels (CLs) given by the comparison of these models to the data are presented in Table 3. Both the default GAL and ARIADNE CR models are excluded by the A_{12}^S distribution, with CLs of $\simeq 10^{-8}$ and $\simeq 10^{-6}$, respectively. The GAL model is also excluded by the A_{qg}^B distribution which gives CL $\simeq 10^{-4}$. The same distribution has a low CL of $\simeq 10^{-2}$ for the ARIADNE CR model. However, ARIADNE, without CR, gives a satisfactory description of all of the distributions. Both versions of HERWIG are completely excluded, with a best CL of $\simeq 10^{-8}$ for no CR and of $\simeq 10^{-9}$ for CR, among all of the asymmetry distributions considered, suggesting that it cannot be used, with confidence, to simulate the soft hadronisation effects that are important for CR studies.[9] Consistent results are obtained by repeating the analysis using the DURHAM $k_\perp$ algorithm [20] with $y_{\mathrm{cut}} = 0.01$ and $y_{\mathrm{cut}} = 0.02$ instead of the JADE algorithm.

Fits are performed to the asymmetry distributions to obtain the best value of R_0 by interpolating the Monte Carlo distributions with different values of R_0. Good fits are obtained, in all cases, with values of R_0 consistent with zero. Further fits are then performed to obtain an upper limit on R_0. Combining the pair of variables A_{12}^B and A_{qg}^B or A_{12}^S and A_{qg}^S, a 95% CL upper limit for R_0 of 0.024 is obtained.

[9] This conclusion does not depend on the size of the systematic uncertainties which, even doubled, would still give HERWIG CLs of $\simeq 10^{-7}$ for the A_{12}^S and A_{qg}^S asymmetries.

7. Summary and conclusions

New observables based on angular separations of particles in the inter-jet regions of symmetric three-jet events are introduced and are found to be very sensitive to CSP and to CR effects.

Upper limits at 95% CL on CSP according to the CS1 and CS2 models of 6.7 and 10.2%, respectively, are obtained. Since the fraction of CSP expected on the basis of the TEVATRON measurements is only 5–10%, after allowing for the effect of gap survival probability, the present analysis is not sufficiently sensitive to confirm or exclude a similar effect in hadronic Z decays.

The GAL model, with the default CR probability, and the ARIADNE CR model are unable to describe the data. Both the no CR and CR versions of HERWIG are completely excluded by the data. However, a good description is provided both by JETSET and the no CR version of ARIADNE. This suggests that the angular asymmetries are also very sensitive to the non-perturbative hadronisation model used. Both JETSET and ARIADNE have similar, string-like, hadronisation models, whereas HERWIG uses cluster fragmentation.

The results presented in this Letter provide important information concerning the systematic uncertainty on the W mass resulting from CR effects as estimated by the GAL, ARIADNE and HERWIG Monte Carlo models. For the default value of the GAL CR parameter, $R_0 = 0.1$, the W mass measured from decays of W pairs into four jets is estimated [9] to be shifted by about 65 MeV. The 0.024 95% CL upper limit obtained in this analysis implies a mass shift of

only a few MeV. Since the default CR models in ARIADNE and HERWIG are unable to correctly describe the Z-decay data, it is difficult to have confidence in their use to describe CR effects in W-pair production.

References

[1] H1 Collaboration, T. Ahmed, et al., Nucl. Phys. B 429 (1994) 477;
ZEUS Collaboration, M. Derrick, et al., Phys. Lett. B 369 (1996) 55.

[2] DØ Collaboration, B. Abbott, et al., Phys. Lett. B 440 (1998) 189;
CDF Collaboration, T. Affolder, et al., Phys. Rev. Lett. 85 (2000) 4215.

[3] M.M. Block, F. Halzen, Phys. Rev. D 63 (2001) 114004;
A.B. Kaidalov, et al., Eur. Phys. J. C 21 (2001) 521.

[4] JADE Collaboration, W. Bartel, et al., Phys. Lett. B 101 (1981) 129;
JADE Collaboration, W. Bartel, et al., Z. Phys. C 21 (1983) 37;
JADE Collaboration, W. Bartel, et al., Phys. Lett. B 134 (1984) 275;
TASSO Collaboration, M. Althoff, et al., Z. Phys. C 29 (1985) 29;
TPC Collaboration, H. Aihara, et al., Z. Phys. C 28 (1985) 31;
OPAL Collaboration, P.D. Acton, et al., Z. Phys. C 58 (1993) 387;
OPAL Collaboration, M.Z. Akrawy, et al., Phys. Lett. B 261 (1991) 334.

[5] L3 Collaboration, M. Acciarri, et al., Phys. Lett. B 345 (1995) 74.

[6] L3 Collaboration, B. Adeva, et al., Nucl. Instrum. Methods A 289 (1990) 35;
M. Acciarri, et al., Nucl. Instrum. Methods A 351 (1994) 300;
M. Chemarin, et al., Nucl. Instrum. Methods A 349 (1994) 345;
I.C. Brock, et al., Nucl. Instrum. Methods A 381 (1996) 236;
A. Adam, et al., Nucl. Instrum. Methods A 383 (1996) 342.

[7] SLD Collaboration, K. Abe, et al., Phys. Rev. Lett. 76 (1996) 4886.

[8] OPAL Collaboration, G. Abbiendi, et al., CERN-EP-2003-031, hep-ex/0306021, Eur. Phys. J.C., submitted for publication.

[9] J. Rathsman, Phys. Lett. B 452 (1999) 364.

[10] ARIADNE Version 4.12 is used, L. Lönnblad, Z. Phys. C 70 (1996) 107.

[11] HERWIG Version 6.202 is used, G. Corcella et al., CERN-TH/2000-284.

[12] L3 Collaboration, P. Achard, et al., Phys. Lett. B 561 (2003) 202.

[13] JADE Collaboration, W. Bartel, et al., Z. Phys. C 33 (1986) 23;
JADE Collaboration, S. Bethke, et al., Phys. Lett. B 213 (1988) 235.

[14] JETSET Version 7.4 is used, T. Sjöstrand, Comput. Phys. Commun. 82 (1994) 74.

[15] PYTHIA Version 6.203 is used, T. Sjöstrand, hep-ph/0108264.

[16] MARK-J Collaboration, D.P. Barber, et al., Phys. Lett. B 89 (1979) 139.

[17] G.C. Fox, F. Wolfram, Phys. Rev. Lett. 41 (1978) 1581;
G.C. Fox, F. Wolfram, Nucl. Phys. B 149 (1979) 413;
G.C. Fox, F. Wolfram, Phys. Lett. B 82 (1979) 134.

[18] S. Banerjee, QCD Studies at L3, Ph.D. Thesis, University of Mumbai, 2000.

[19] The L3 detector simulation is based on GEANT Version 3.15, R. Brun et al., CERN DD/EE/84-1, 1984, revised 1987. GHEISHA program, H. Fesefeldt, RWTH Aachen Report PITHA 85/02, 1985 is used to simulate hadronic interactions.

[20] N. Brown, W.J. Stirling, Z. Phys. C 53 (1992) 629;
S. Catani, et al., Phys. Lett. B 269 (1991) 432;
S. Bethke, et al., Nucl. Phys. B 370 (1992) 310.